

Base resistance of screw displacement piles in sand

Kevin Duffy¹, Ken Gavin², Mandy Korff³, Dirk de Lange^{1,4}

¹Ph.D. Candidate, Department of Geoscience & Engineering, TU Delft, The Netherlands

(corresponding author). Email: k.duffy@tudelft.nl

²Professor of Subsurface Engineering, Department of Geoscience & Engineering, TU Delft, The Netherlands

³Associate Professor in Geotechnical Practice, Department of Geoscience & Engineering, TU Delft, The Netherlands

⁴Geotechnical Researcher, Deltares, Delft, The Netherlands

ABSTRACT

Full-scale axial load tests were performed on five screw injection piles founded in medium dense to dense sand at a site in Delft, the Netherlands. Each pile was instrumented with distributed fibre optic sensors along its full length, giving detailed insights into the shaft and base response under compression loading. The paper focusses on the pile base response and combines the test results with a newly compiled database of instrumented load tests on screw displacement piles in sand. Given the range of screw displacement piles on the market, the influence of different installation methods and pile geometries on the base resistance can be assessed through the database. In summary, the analysis showed that all screw displacement pile types tended to mobilise base capacities similar to bored or non-displacement piles. Despite high variability in the database, no significant trend with pile geometry, such as length or diameter, was evident.

INTRODUCTION

Screw displacement piles, also known as drilled displacement or auger displacement piles (Basu et al. 2010), include pile types such as the Atlas, FDP, Fundex, Olivier and Omega piles. These piles are installed using both torque and a push-in force. Unlike bored piles, continuous flight auger (CFA) piles or screw anchors, screw displacement piles displace the soil radially away from the pile shaft and underneath the pile base, minimising the degree of soil transportation. Generally, this is assumed to be favourable for the ultimate pile capacity, implying that screw displacement piles provide comparatively high capacities whilst producing low noise and vibration during installation.

Design methods for screw displacement piles often use the cone penetration test (CPT) to determine the pile base resistance in sand (Kempfert and Becker 2010; Huybrechts et al. 2016; van Seters 2016; Moshfeghi and Eslami 2019; Gavin et al. 2021). These methods define the ultimate base capacity $q_{b0.1}$ at a base displacement of 10% of the pile diameter D using the equation:

$$q_{b0.1} = \alpha_p q_{c,avg} \quad (1)$$

where α_p is an empirical correlation factor and $q_{c,avg}$ is a weighted average of CPT cone tip resistances in a diameter dependent zone around the pile base. There is no universally accepted means of determining $q_{c,avg}$ and the different methods available can lead to variability in the derived α_p . Methods for determining $q_{c,avg}$ include the Dutch 4D/8D method (van Mierlo and Koppejan 1952; Reinders et al. 2016) and the LCPC 1.5D method (Bustamente and Gianceselli 1982), developed at Laboratoire Central des Ponts et Chaussées (LCPC). Yet research (van der Linden et al. 2018, Lehane 2019) has suggested that both methods do not adequately describe the different penetration mechanisms that affect the measured cone resistance, particularly in very variable soils. The recently developed “filter method” (Boulanger and DeJong 2018) uses an inverse filtering technique to derive the true cone resistance and has been shown to improve on existing averaging methods when applied to pile design (Bittar et al. 2022; de Boorder et al. 2022).

Much of the early development and research into screw displacement piles and CPT-based design occurred in the Netherlands and Belgium (Basu et al. 2010; Bottiau and Huybrechts 2019). In these

countries, screw displacement piles in sand are designed using relatively high α_p factors. For example, the Dutch design code (NEN 2017) prescribes an α_p of 0.63 when $q_{c,avg}$ is determined by the 4D/8D averaging method. In this case, the α_p is much closer to that of a driven closed-ended pile ($\alpha_p = 0.70$) compared to that of a bored pile ($\alpha_p = 0.35$). Essentially, the high α_p implies that screw displacement pile installation improves the stress state around the pile base and so the pile performs more like a fully displacing pile than a non-displacing pile.

Precisely quantifying this beneficial effect is challenging. Laboratory tests (Slatter 2000) has shown how soil is displaced downwards and radially away from the drilling tool of a screw displacement pile, a phenomenon controlled by both the drilling tool geometry and installation parameters, such as the rotational speed and pulldown force. Numerical analyses (Pucker and Grabe 2012, Basu et al. 2014, Knappett et al. 2014) have also supported these findings, showing increased soil densification up to one to three pile diameters away from the pile shaft. However, the mechanisms occurring around the pile base are also affected by direct transport of soil up the screw flights, particularly when the displacement body of the pile is offset away from the pile base, like in the case of Omega piles (Slatter 2000). Translating these models to full-scale piles brings another layer of complexity. When the hollow drilling tool is filled with wet concrete and subsequently withdrawn, another series of stress changes and re-equalisation are initiated (Bustamente & Gianceselli 1998; van Impe 2001), potentially leading to a non-uniform pile base in terms of both geometry and stiffness.

Efforts have been made to translate installation parameters into a predicted load capacity for screw displacement piles (NeSmith 2003; Krasinski 2023), although caution is advised when using these methodologies because of the limited research and data available (Basu et al. 2010). Therefore, CPT-based approaches remain the most reliable way of assessing screw displacement pile capacity. Several database approaches (De Cock 2008; Basu et al. 2010; Jeffrey 2012; Park et al. 2012; Larisch 2014; Moshfeghi and Eslami 2019; Figueroa et al. 2022) have been performed to assess the reliability of different design methods. Nevertheless, a comprehensive database assessment of the pile base response is still lacking because of the limited number of fully instrumented static load tests, especially tests paired with a neighbouring CPT that would allow α_p values to be derived. Recent tests on screw

displacement piles in very dense sand (Duffy et al. 2024) and soft clay (Siegel et al. 2019) have suggested an α_p factor much lower than currently prescribed in design standards.

To investigate the base resistance of screw displacement piles in sand, this paper first presents the results of static load tests on five instrumented screw injection piles, a type of screw displacement pile commonly used in the Netherlands and Belgium. Each pile was instrumented with distributed fibre optic sensors, giving detailed insights into the geotechnical and structural response of the piles. The test results were then combined with a newly compiled database of instrumented load tests on screw displacement piles founded in sand. Using the database, the paper shows the importance of averaging methods in CPT-based design formulations for the pile base resistance and compares the base response of different screw displacement pile types to investigate if different installation methods have an influence on the ultimate pile base response.

BACKGROUND OF SCREW INJECTION PILES

Screw injection piles are a type of screw displacement pile which use an injection fluid during pile installation, simultaneously with a push-in force and torque. The fluid is injected from the pile tip, passing along the pile shaft and out through an annular space around the pile at the ground surface, reducing the resistance acting on the pile shaft and on the pile tip. If grout is used as the injection fluid, an outer shell is created around the pile upon grout hardening, filling the annular space and increasing the pile's cross-sectional area. Overall, this means the pile type is quite adept at installing in dense sand and variable deposits, whilst still generating low noise and vibrations. These reasons, for instance, are why screw injection piles are steadily becoming more and more common in the Netherlands and Belgium (Bottiau and Huybrechts 2019).

Precisely how screw injection piles are installed varies from contractor to contractor. Variations can include screw tip shape, grout properties, the location of the injection outlet or with how the casing is extracted. Two common screw injection pile types include the *Fundex* and *Tubex* systems, both of which can be installed with or without injection. A key installation characteristic of Fundex piles (**Fig. 1**) is the thick-walled reusable steel casing with a sacrificial screw tip. Tubex piles, on the other hand, use a thin-walled sacrificial steel tube with a screw tip permanently welded to the bottom. Because the tube

remains in-situ, a reinforcement cage is often not needed and so after installation, the steel tube is filled with just concrete.

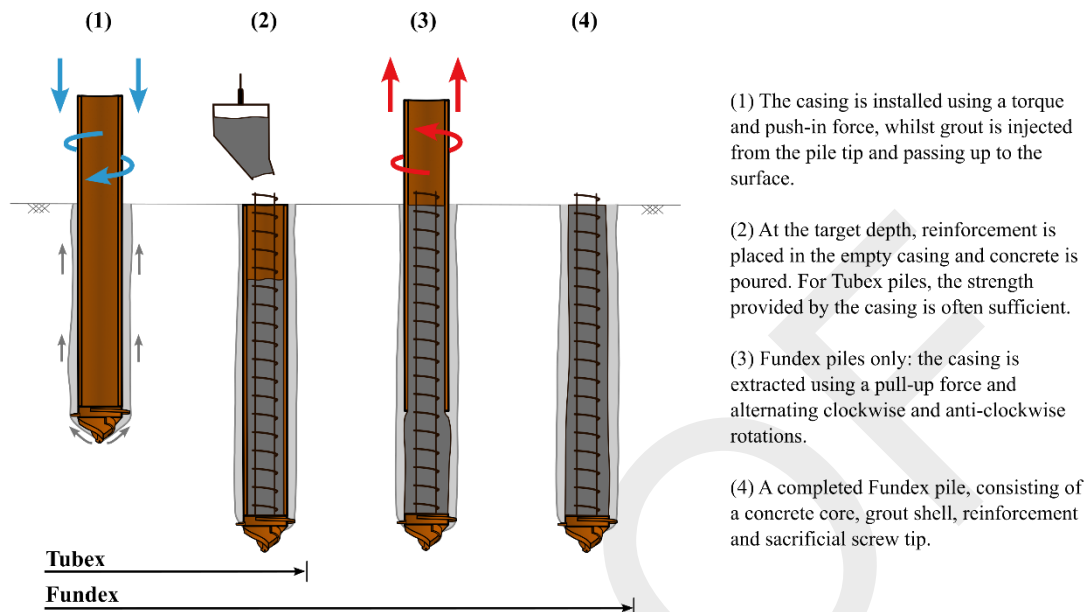


Fig. 1. Installation of a Fundex and Tubex pile with grout injection.

The combined screwing and injection makes it challenging to understand how different pile sizes, screw tip shapes and installation parameters (e.g. penetration rate, pulldown force, revolutions per minute, grout flow rate, grout pressure, grout water-cement ratio) affect the base and shaft response under axial loading, particularly given the interdependencies between the parameters. An increased pulldown force, for instance, increases the penetration rate and subsequently requires an increased grout flow rate to maintain the grout body around the pile. Admiraal et al. (2022) performed tension load tests in the field on fifteen scaled screw injection piles, investigating how grout injection parameters such as flow rate and water-cement ratio affected the pile shaft resistance. The results indicated that different water-cement ratios in the grout mixes did not create any observable changes in the piles' tensile capacities, although higher grout flow rates may lead to lower ultimate shear stresses. The static load tests performed in the very dense sands of the port of Rotterdam (Duffy et al. 2024), use both discrete and distributed fibre optic sensors to provide comprehensive measurements of the normal force along the entire pile length of three screw injection piles. Compared to the full-displacement driven closed-ended piles tested at the same site, the screw injection piles exhibited a much softer base stiffness and

mobilised an α_p of just 0.30. The low α_p values mobilised initiated the test programme presented in this paper to see if site-specific effects such as soil conditions or installation procedures affected the base response.

EXPERIMENTAL PROGRAMME

Ground conditions

Pile installation and testing was performed in early 2022 at the Flood Proof Holland test site of Delft University of Technology. Six screw injection piles were installed, spaced at least four metres apart (Fig. 2). Prior to installation, four CPTs were performed within two metres of each pile location. The upper two metres of the site was a made ground fill composed of coarse sand, gravel and cobbles. Underneath this were six metres of soft Holocene clay with CPT cone resistances of around 0.2 MPa (Fig. 3), underlain by a two-metre-thick medium-dense sand layer and a three-metre-thick firm clay layer. The test piles extended through these layers and down to a medium dense to dense sand layer located 16 m below ground level. This founding layer had cone tip resistances between 10 to 25 MPa, with an average value of around 15 MPa. Geologically, this sand layer is referred to as the Kreftenheye Formation and is widespread across much of the western Netherlands and the Dutch North Sea sector (Rijsdijk et al. 2005; Hijma et al. 2012).

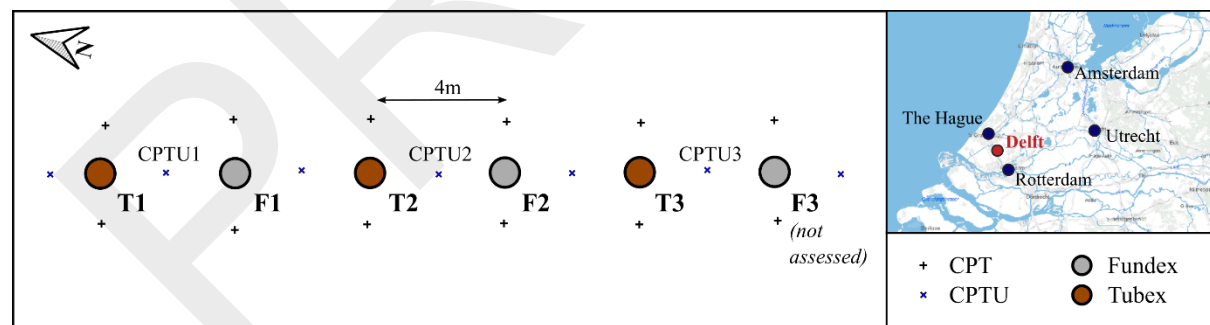


Fig. 2. Layout and location of the Delft test site (inset map courtesy of <http://www.pdok.nl>).

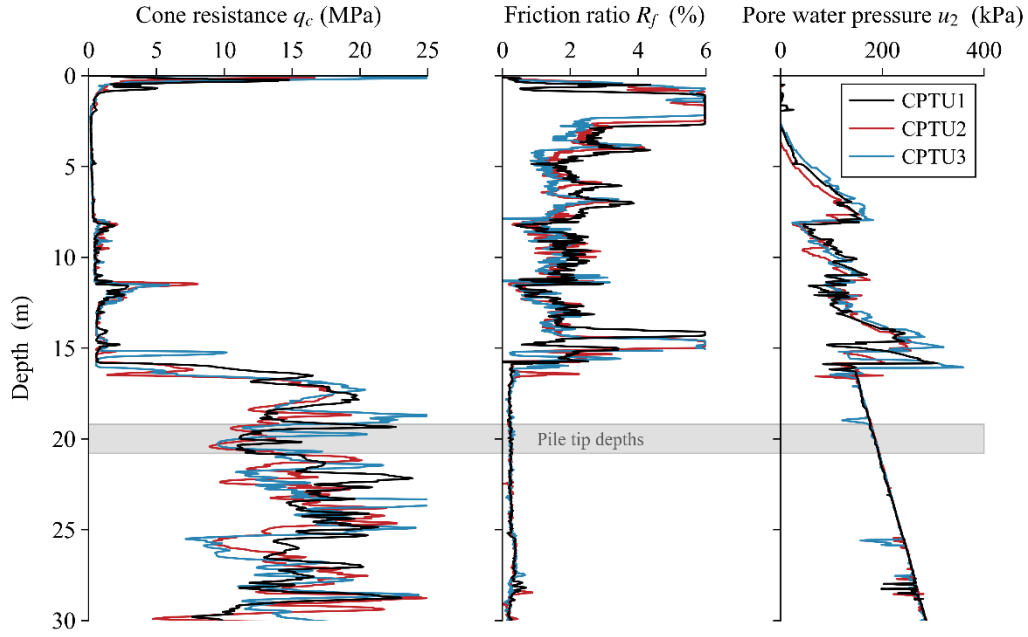


Fig. 3. Selected CPTs from the test site.

Pile geometry & installation

Three Fundex piles (F1, F2 and F3) and three Tubex piles (T1, T2 and T3) were installed by the contractor Fundex Piling Group to compare the base and shaft response of two different types of screw injection piles under similar site conditions. Both pile types had identical screw tips (**Fig. 4**), each with a single helical screw flange measuring 470 mm at its outermost diameter. Two injection outlets were located in these tips, facing in opposite directions. These outlets injected grout with a water-cement ratio of 1.5 until just above the target depth, from which point the piles were screwed in an additional 25 cm without any grout injection.

The Fundex piles were installed by a reusable casing with an outer diameter of 380 mm and a wall thickness of 32 mm. The soft upper clay layer increased the risk of pile bending and structural failure, particularly in the event of eccentric loading. To mitigate this risk, a single H-beam profile (HEB 160) was used as reinforcement in the Fundex piles and was placed in the reusable casing before concrete pouring, resting directly on the screw tip. For the Tubex piles, each screw tip was welded to a sacrificial tube with an outer diameter of 382 mm and a wall thickness of 13 mm. Because the tube remains in situ, a reinforcement cage is often not needed and so only concrete is placed in the tube after installation. All piles were filled with C45/55 concrete.

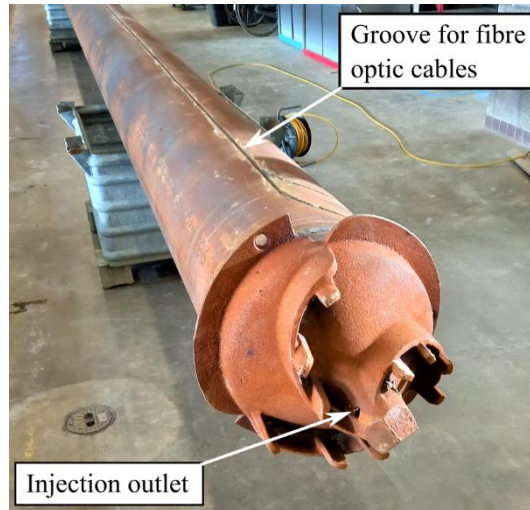


Fig. 4. Screw tip of the Tubex piles.

A key consideration in the installation of screw injection piles is balancing the incoming and outcoming grout flow rate, helping to reduce the installation resistance and to create a continuous grout shell around the pile. During installation of the first pile, pile T1, no grout outflow was observed at the ground surface despite the constant rate of incoming grout at 120 L/min (**Fig. 5**). This suggests that some of the grout may have percolated through permeable soil layers or created enlarged areas of the pile shaft in the softer layers. For the remaining Tubex piles, the penetration velocity was reduced through the upper layers and the grout flow rate was increased to 180 L/min to encourage more grout outflow, but no grout outflow was subsequently observed. The Fundex piles used the same incoming grout flow rate as piles T2 and T3, albeit with an increased penetration velocity to reduce the risk of the screw tip dislodging from the casing during penetration. Grout outflow was observed for piles F1 and F2 across the lower sand layer but no outflow was observed across this layer for pile F3. Subsequent problems with extracting the reusable casing of pile F3 meant that the pile was of insufficient quality to be considered a suitable test pile. As a result, pile F3 has not been considered further in this paper.

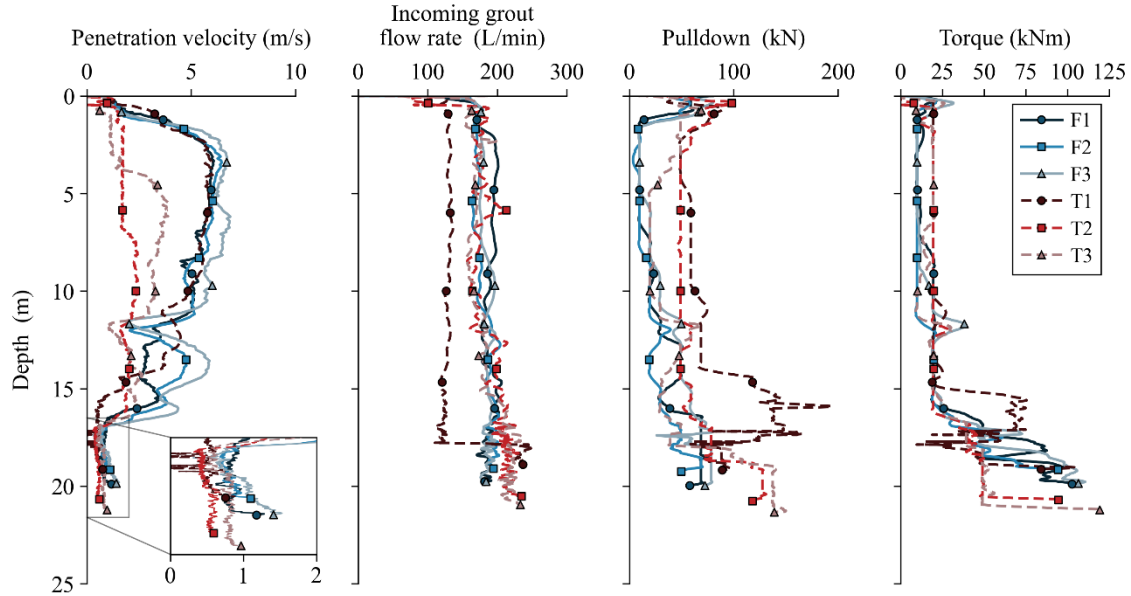


Fig. 5. Installation data of the six test piles.

Table 1. Overview of the test piles.

Pile	Diameter D (mm)	Length L (m) ^a	$q_{c,LCPC}$ (MPa) ^b	Pile age (days)
F1	470	20.0	12.6	65
F2	470	19.2	13.5	70
F3 ^c	470	20.0	10.9	n/a
T1	470	19.9	11.9	64
T2	470	20.3	11.7	68
T3	470	20.8	15.4	73

^a The pile base elevation was defined as the shoulder of the conical tip (35 cm in height).

^b Weighted cone resistance around the pile base, determined using the 1.5D LCPC method (Bustamente and Gianceselli 1982)

^c Test results of pile F3 not assessed because of problems with casing extraction

Strain instrumentation

All piles were instrumented along their full length with steel-reinforced fibre optic cables. For the Fundex piles, the fibre optic cables were glued to the H-beam reinforcement at its two flanges and in the centre of the web. For the Tubex piles, two 5 mm deep grooves were formed in the outside of the casing (**Fig. 4**) into which a fibre optic cable was glued. Both pile types were instrumented in an indoor, temperature-controlled environment and the steel was scoured and degreased before gluing with two-part epoxy.

During load testing, the cables were interrogated using Brillouin Optical Frequency Domain Analysis (BOFDA) through a fibrisTerre fTB 5020 interrogator. This process gave a continuous profile of strain

along the length of the pile at a spatial resolution of 20 cm and at a frequency of every 90 seconds. Strain readings were then converted to a normal force based on the stress–strain response of the upper part of the pile and using the tangent and secant stiffness method described by Fellenius (2001). The measured stiffness response agreed well (**Fig. 6**) with the theoretical initial stiffness—derived using the composite steel-concrete-grout stiffness and assuming a grout stiffness of 10 MPa and a shaft diameter of 470 mm. As expected, a slight degradation in stiffness with increasing strain is visible across most of the piles. The only outlier is pile F2, which shows an apparent strain-hardening response with increasing strain. Variations in stiffness are inevitably expected along the length of the pile because of potential changes in material strength and pile diameter. However, since the piles were not extracted following testing, a constant stiffness has been assumed for the entire length of the pile.

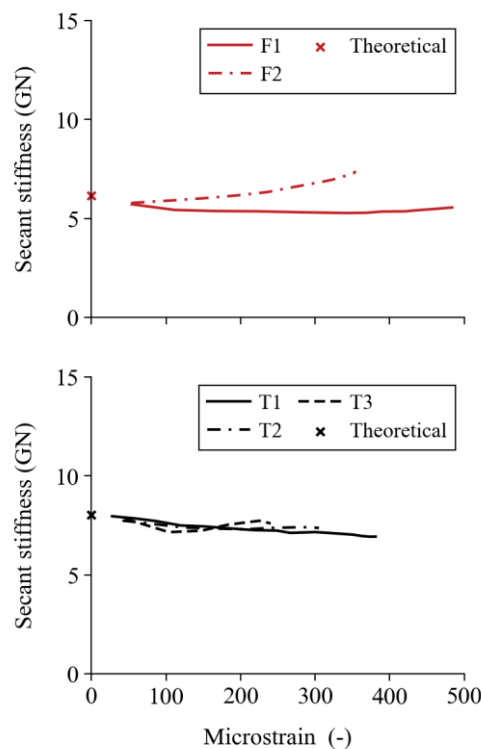


Fig. 6. Secant stiffness measured by the uppermost strain readings in each pile.

Load test procedure

All piles were subjected to stepwise, axial compression loads using a single hydraulic jack and a reaction provided by kentledge. The standard duration of each load step was at least thirty minutes, the duration of which was extended if the creep rate of the pile head exceeded 1.2 mm/s. Each load step was either

prolonged or advanced to the next step depending on the creep rate of the pile head and the duration of the existing load step, with each step lasting at least thirty minutes. To measure the pile head displacement, four potentiometers were installed around the pile head and measured with respect to two wooden reference beams either side of the pile. These displacement measurements were also cross-checked by two different automatic levelling stations, located around 10–20 m away from the pile. A steel rod known as a telltale was left free-standing in a tube within each pile, resting directly on the pile tip. By measuring the change in elevation of the top of the telltale with respect to the pile head, the elastic compression of the pile body could be deduced and so the telltale acted as a supplement to the BOFDA strain measurements. The maximum deviation between the telltale and BOFDA measurements of the elastic displacement was around 1–2 mm for each test, with the exception of the test on pile T2 where a deviation of up to 6 mm occurred. It is surmised that this is as a result of movement and bending of the telltale within its housing, resulting in a higher (apparent) elastic displacement compared to the other piles.

The piles were unloaded once the pile base displacement reached at least $0.1D$, referred to as the pile failure load. Thereafter, an attempt was made to reload the pile to this failure load.

LOAD TEST RESULTS

Load-displacement response

All piles showed very similar load-displacement responses up to a load of around 1.2 MN (**Fig. 7**). From this point, piles F1, F2 and T1 reached maximum loads of approximately 2.6 MN, each exhibiting rapid plunging failure and bringing the piles to the $0.1D$ failure criterion. Load cycles at the end of the initial tests failed to return to these maximum loads. Up until a load of 2.3 MN, pile T2 responded similarly to these three piles. However, one hour into this load step, the pile displaced suddenly and the hydraulic pump could not pump quickly enough to sustain the 2.3 MN load. Subsequent load cycles could not reach loads greater than 1.5 MN because of the high displacement rate of the pile. On the other hand, the behaviour of pile T3 was notably different to the other piles: the pile exhibited high creep rates during maintained load steps from 1.0 MN onwards. The pile reached the $0.1D$ failure

criterion at a maximum load of 1.7 MN, with very large pile head displacements occurring at this load.

In the subsequent reload cycle, the pile reached peak loads similar to the load at failure.

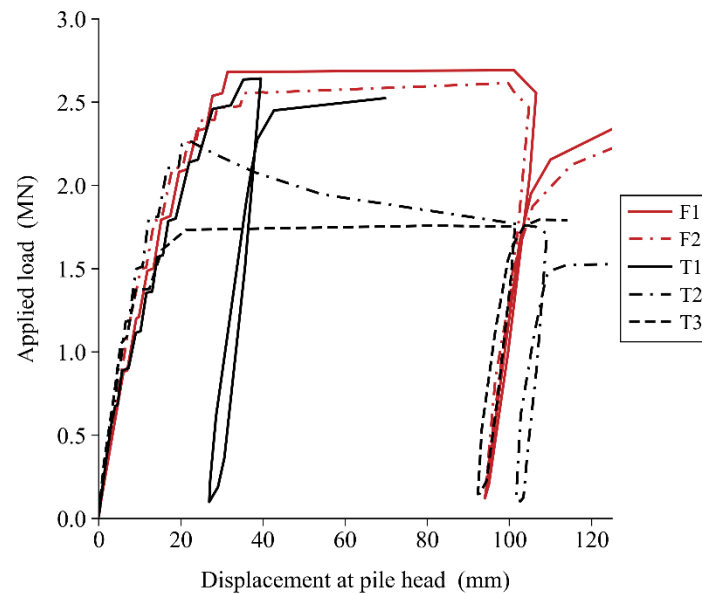


Fig. 7. Load-displacement response under axial compressive loading

Load distribution

The measured axial force distribution with depth shows several distinct features (**Fig. 8**). All five piles transferred little of the applied load to the soft clay in the first 8 m below the surface. From 8 m to 16 m, the higher shaft resistance of the medium dense sand and firm clay led to a greater reduction in the axial force compared to the soft clay. Piles F1 and F2 showed localised deviations in the measured load across this zone, particularly when compared to the Tubex piles. These deviations can potentially be explained by the removal of the steel tube of the Fundex piles, increasing the chance of localised changes in pile stiffness or cross-sectional area.

The load distribution distinctly changes at the boundary of the lower sand layer at 16 m depth. At this boundary, the apparent axial force in piles F1, F2 and T1 reduces rapidly with depth to the pile base. Contrastingly, piles T2 and T3 show a different pattern. Taking pile T2 for instance, the load distribution is similar to that of pile T1 up until a load of 2.0 MN. However, one hour into the 2.0 MN load step, sudden displacement of the pile led to a corresponding reduction in its total capacity. When the pile reached an equilibrium at 1.5 MN, the slope of the load distribution appeared to have changed in the

lower sand layer (**Fig. 8**). Little to no reduction in load was exhibited across this layer, implying that little shear resistance could be mobilised. This same effect is also shown in pile T3 for applied loads greater than 1 MN. Beyond this load, high creep rates were observed at the pile head during load-holding periods.

It is likely that structural failure occurred in Tubex piles T2 and T3 because of a shear failure in the grout body itself or adhesive failure at the grout–steel interface, similar to that described by Duffy et al. (2024). The structural failure meant little shaft friction could develop in the lower sand layer, reducing the total capacity of T2 and T3 by 0.5 MN (**Fig. 7**). This reduction in total capacity corresponds to the total load taken by the lower sand layer in piles T1, F1 and F2—piles which showed no evidence of structural failure in their measured load distributions (**Fig. 8**). During installation, no return grout flow was observed in all three Tubex piles, suggesting that local hydrogeological conditions may have affected the development of the grout body—namely the soft impermeable clay overlying medium dense to dense sand. For future test sites or projects, a reduced water–cement ratio may improve the shear resistance and adhesive resistance of the grout, although site-specific dummy piles are recommended to verify that the mix provides sufficient fluidisation.

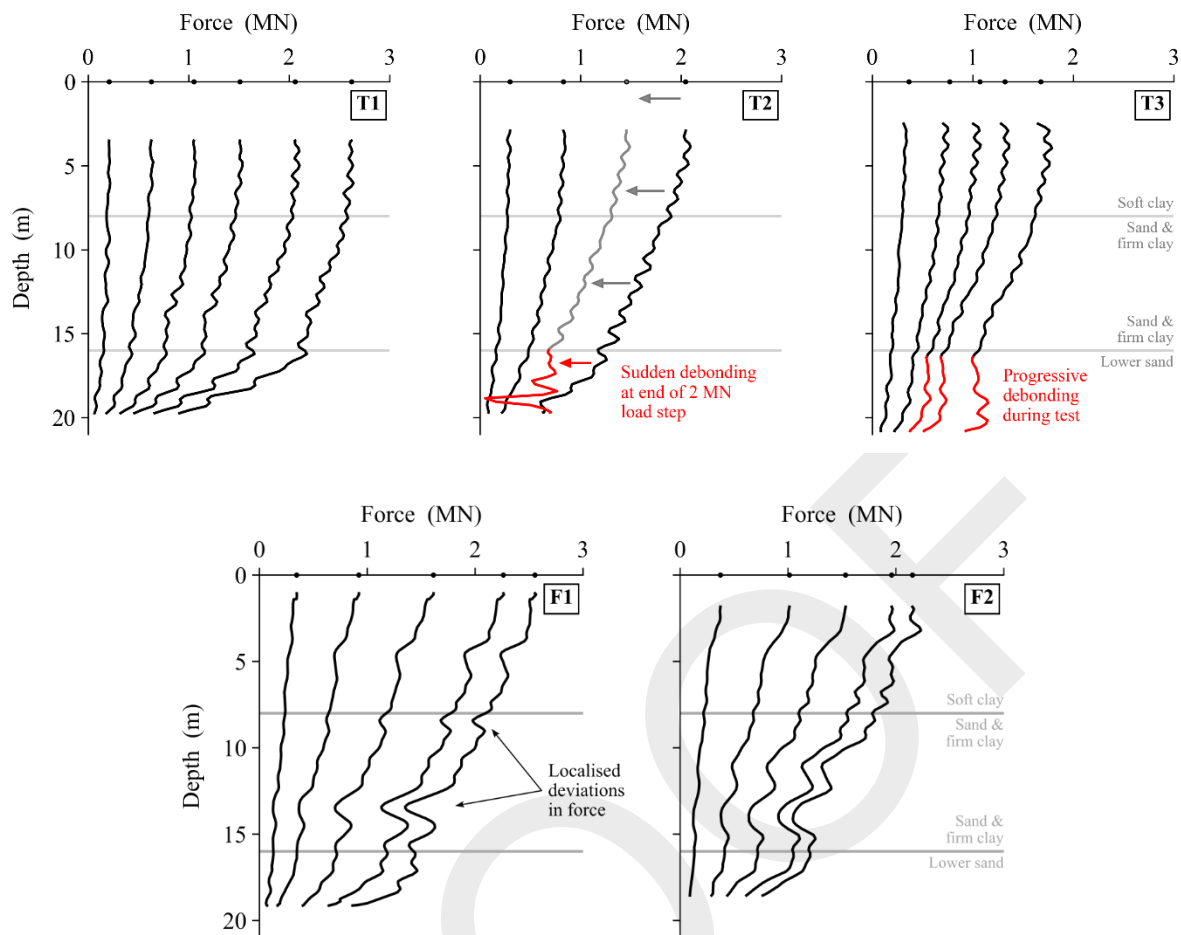


Fig. 8. Axial force distribution measured by the BOFDA system during each test. Readings by a load cell on top of the pile are given by discrete points.

Shaft resistance

While the paper primarily focusses on the base resistance of the test piles, the measured shaft resistance in the lower sand layer is presented in **Fig. 9** to fully understand the response of the piles in the primary load-bearing layer. The two Fundex piles, F1 and F2, mobilised maximum shaft resistances of 225 kPa at displacements between 15 and 25 mm. Both piles show post-peak softening with increasing displacement, reducing the shaft resistance to between 150 and 200 kPa. Tubex pile T1 also mobilised its resistance at a similar rate to the Fundex piles, reaching a maximum value of 240 kPa. However at this resistance, the pile was unloaded and so no clear softening could develop in the shaft response. Lastly, piles T2 and T3 reached maximum shaft resistances of only 175 kPa and 15 kPa respectively in the lower sand layer before debonding occurred at the grout-steel interface.

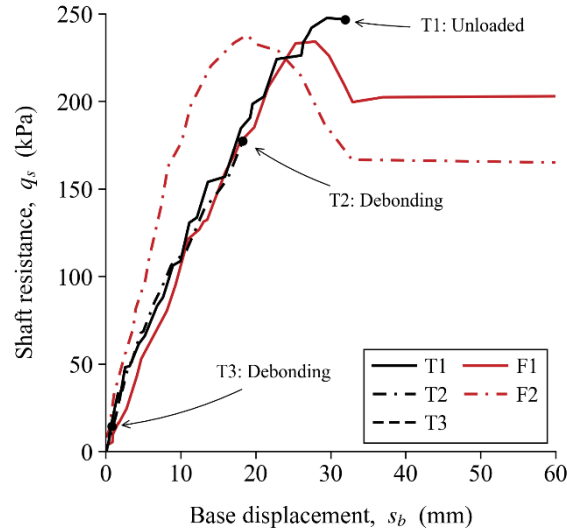


Fig. 9. Shaft response of the test piles in the lower sand layer.

Base resistance

To determine the base resistance, the load distribution was extrapolated to the pile base from the lowermost strain reading, a reading always within one pile diameter from the pile base. To convert from a resistance to a stress, the maximum diameter of the helical screw was used (=470 mm). Grout injection stopped 25 cm prior to the pile reaching its final depth, so it is assumed that no grout is present underneath the screw tip.

The base resistances mobilised by piles T1, T2, F1 and F2 were very similar until a pile base displacement of 15 mm (**Fig. 10**). After this point, the responses diverged: pile T1 reached the highest resistance of 5 MPa, pile T2 the lowest of 2.5 MPa and the two Fundex piles reached resistances in between these two extremes. The third Tubex pile, pile T3, appeared to behave much stiffer than the four other piles, although its response may have been affected by the structural failure of the grout body early on in the test. Ultimately, pile T3 yielded a maximum base resistance of 5 MPa, similar to pile T1.

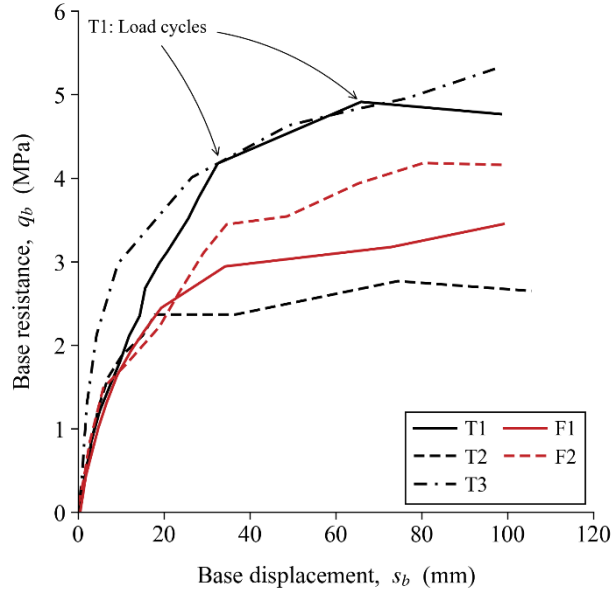


Fig. 10. Measured base response of the test piles.

To account for variations in soil conditions around the pile base, the base resistances have been normalised by the LCPC averaging method $q_{c,LCPC}$ (Bustamente and Gianceselli 1982) shown in **Fig. 11**. At a pile base displacement of 10% of the pile diameter, the normalised resistances (that is, α_p from Eq. 1) are between 0.20 and 0.30 for four of the five piles. Additional gains in capacity are marginal at displacements beyond $0.1D$. The only exception is pile T1, which reached an α_p of around 0.40. During installation, no grout injection was performed over the final 25 cm, meaning that any installation-induced changes in the mobilised α_p is more likely to be related to parameters such as penetration velocity or torque. However, no clear correlations can be drawn between the measured installation data (**Fig. 5**) and the normalised base resistance (**Fig. 11**).

Considering standard-specific averaging methods, the α_p factors range from 0.25 to 0.45 when using the 4D/8D averaging method prescribed by the Dutch standard (van Mierlo and Koppejan 1952; NEN 2017) and from 0.30 to 0.45 using the de Beer method (de Beer 1971) in the Belgian standard (NBN 2022). These mobilised values are much closer to the α_p values of a non-displacement pile where α_p ranges from 0.25 to 0.50 in both standards. This suggests that pile installation at the Delft test site

created little to no improvement in the pile base resistance, performing similarly to a low displacement pile or a bored pile.

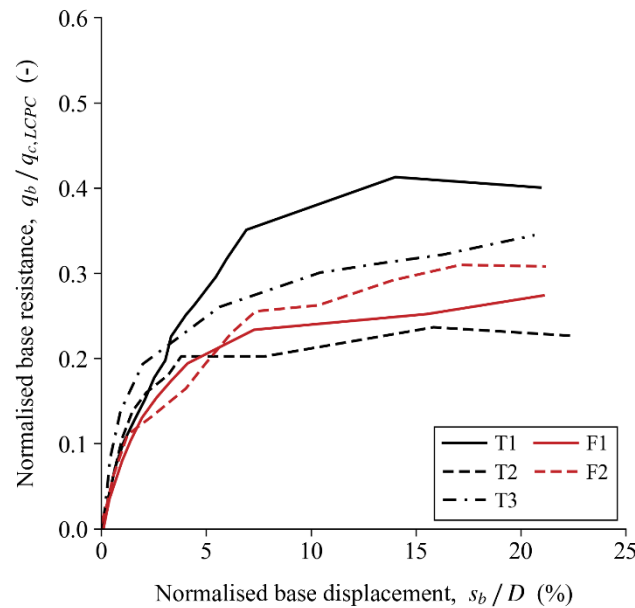


Fig. 11. Normalised base response using the LCPC 1.5D averaging method.

DATABASE ASSESSMENT

A database of screw displacement pile tests was compiled to investigate if site-specific ground and installation procedures affected the pile response. The database comprises at least 200 static load tests on screw displacement piles founded in sand. In addition to the screw injection piles, the other screw displacement piles have been categorised into three types:

- Smooth shaft:** Pile is installed with a sacrificial screw tip larger than the steel casing. The casing can remain in-situ, or else it is filled with concrete and extracted, leaving the screw tip behind. The result is a relatively smooth shaft with a screw tip at the pile base. Common pile types include the first generation of Fundex piles without grout injection, such as that described in Basu et al. (2010).
- Helical shaft:** The pile is installed using a steel drilling tool with a screw head. A sacrificial base plate or pointed tip is fitted to the bottom of the drilling tool to prevent groundwater ingress. Once the target depth is reached, the drilling tool is filled with concrete and is extracted

at a rate which matches the pitch of the helical screw, creating a screw shaped shaft. Well-known pile types include the Atlas or Olivier pile types.

- **With displacement body:** the pile is constructed using a drilling tool with several screw flights either side of an oversized displacement body that is several diameters away from the pile base. Similar to helical-shafted screw displacement piles, the drilling tool is fitted with a base plate at the bottom. Once the target depth is reached, the drilling tool is filled with concrete and extracted, with the displacement body creating a relatively smooth shafted pile. Pile types with displacement bodies generally have varying screw and displacement body geometries, examples of which include the De Waal and Omega piles.

From this database, twenty-four piles were selected to compare the influence of installation methods on the ultimate pile base response (**Table 2**). Each test directly measured the pile base resistance and loaded the pile to displacements of at least 5% of the pile diameter. At least one CPT was performed near each pile, giving a clear profile of the soil stratigraphy around the pile base. The outermost diameter was used to determine the pile base resistance—generally the width of the helical flange at the screw tip.

Table 2. Database of static load tests on screw displacement piles in sand, where the base resistance was directly measured.

ID	Site and pile	Pile Type	D^a (mm)	Length (m)	$S_{b,max}/D$ (%)	$q_{b,0.1}^b$ (MPa)	$q_{c,LCPC}$ (MPa)	$q_b/q_{c,LCPC}$	Reference
Smooth shaft									
1	Beemster P2	Fundex ^c	150	2.9	28	7.0	15.7	0.45	(van der Geest et al. 2020)
2	Beemster P3	HEK pile ^c	150	2.9	27	7.0	32.9	0.21	(van der Geest et al. 2020)
3	Beemster P6	Fundex ^c	150	2.9	25	8.4	22.5	0.37	(van der Geest et al. 2020)
4	Beemster P7	HEK pile ^c	150	2.9	29	7.0	32.6	0.21	(van der Geest et al. 2020)
Helical shaft									
5	Zeeland O1	Olivier	460	9.1	14	3.4	22.8	0.15	Personal database
6	Zeeland O2	Olivier	460	8.0	11	5.9	23.2	0.25	Personal database
7	Zeeland O3	Olivier	460	9.5	14	6.5	20.6	0.32	Personal database
With displacement body									
8	Elblag P9	DPDT	400	7.5	6	3.7	15.6	0.24	(Krasiński and Wiszniewski 2021)
9	Grottgera P600	SDP	400	11.0	10	3.0	10.7	0.28	(Krasiński 2023)
10	Loenhout S2	Omega	410	9.5	14	2.8	9.9	0.28	(Theys et al. 2003)
11	Lomme	De Waal	360	8.5	9	5.2	25.3	0.21	(Bustamente and Ganeselli 1997)
12	Oostende	Omega	460	21.6	10	4.2	30.1	0.14	(Van Impe et al. 2013)

13	Pruszcz b1	SDC	356	7.5	5	4.0	10.2	0.39	(Kraśiński 2011)
14	Zulawy P6293	CMC	400	12.6	11	2.6	9.6	0.27	(Kraśiński and Wiszniewski 2021)
Screw injection									
15	Amaliahaven SI1	Tubex	850	37.0	11	9.6	36.1	0.27	(Duffy et al. 2024)
16	Amaliahaven SI2	Tubex	850	37.1	12	10.5	53.7	0.20	(Duffy et al. 2024)
17	Amaliahaven SI4	Tubex	850	34.1	12	9.9	46.5	0.21	(Duffy et al. 2024)
18	Delft F1	Fundex	470	20.0	23	3.0	9.9	0.24	This paper
19	Delft F2	Fundex	470	19.2	23	3.5	8.9	0.26	This paper
20	Delft T1	Tubex	470	19.9	23	4.8	9.5	0.40	This paper
21	Delft T2	Tubex	470	20.3	26	2.4	9.1	0.20	This paper
22	Delft T3	Tubex	470	20.9	22	4.7	12.2	0.30	This paper
23	Haren	Fundex	660	16.4	8	8.2	15.1	0.54	(Bottiau and Huybrechts 2019)
24	Rosmalen P3	Tubex	400	7.4	22	1.4	10.5	0.13	(Geerling and Janse 1992)

^a The outer diameter of the pile at the pile tip was used.

^b If $5\% \leq s_b / D \leq 10\%$, extrapolation to 10% was performed using the method by Chin (1970).

^c The tests at Beemster were scaled versions of existing pile types. No grout injection was applied.

Note: CMC = Controlled Modulus Column; DPDT = Displacement Pile Drilling Tool; SDC = Soil Displacing Column; SDP = Soil Displacing Pile.

Influence of partial embedment

It is well-documented that the tip resistance of a pile and a CPT cone depends on the soil conditions within a zone above and below the tip (Ahmadi and Robertson 2005; White and Bolton 2005; Xu and Lehane 2008; de Lange 2018; van der Linden et al. 2018; Tehrani et al. 2018). These soil conditions can be accounted for in design using so-called averaging methods. For instance:

- The **4D/8D method** (van Mierlo and Koppejan 1952; Reinders et al. 2016), also known as the Dutch method or the Koppejan method, assumes a Prandtl-wedge failure mechanism in sand, propagating into a logarithmic spiral shaped failure mechanism up to four pile diameters below the pile tip and eight pile diameters above the pile tip. To derive $q_{c,avg}$, the method combines the weighted average of q_c values in this zone with a minimum path rule—a rule which essentially prioritises the effect of weak layers on $q_{c,avg}$. The method is proposed in the Unified design method for driven piles in sand (Lehane et al. 2020) as well as in the Netherlands (NEN 2017) where α_p for screw displacement piles is 0.63.
- The **De Beer method** is based on the averaging method developed by Meyerhof (1959) which assumes a logarithmic spiral failure plane like the 4D/8D method. De Beer (1971) updated the method with an analytical approach that takes the scaling effect into account between a CPT

and a pile. The De Beer method is popular in Belgium where screw displacement piles are widely used and researched, most notably the test campaigns on screw displacement piles at Limelette (Huybrechts and Whenham 2003) and Sint-Katelijne-Waver (Huybrechts 2001). Using the De Beer method, the Belgian standard (NBN 2022) prescribes an α_p of 0.50.

- The **LCPC 1.5D method** (Bustamente and Gianceselli 1982) simply averages the q_c values in a zone 1.5 pile diameters above and below the pile tip, limiting the q_c values to $\pm 30\%$ of the arithmetic average. The LCPC method is generally considered the most common averaging method (Bittar et al. 2022) and is used in the French design method (AFNOR 2018; Verheyde and Baguelin 2019) where α_p is 0.50 for screw displacement piles, assuming a penetration of at least five pile diameters into the load-bearing layer.
- The **adapted filter method** (de Boorder, de Lange and Gavin 2022) is a simplification of the filter method by Boulanger and DeJong (2018) and is calibrated against penetrometer tests in interlayered soils (de Lange 2018). In general, the filter method aims to correct for the influence of weak layers on the base resistance by using two weighting factors: one factor accounting for the distance from the pile base and the second factor accounting for differences in soil strength. The filter method itself has been shown to improve on existing averaging methods when analysed in laboratory and field tests (Bittar, Tian and Lehane 2022) and is recommended for use in the recently developed Unified design method for driven piles in sand (Lehane et al. 2020).

Fig. 12 compares the α_p from these four different averaging methods to the normalised distance L_p/D between the pile base and an overlying clay layer, referred to as the pile embedment into sand. Across the dataset, the mean α_p using the 4D/8D and De Beer methods is 0.48 and 0.60 respectively. Crucially, the mean value is affected by high variation in α_p at low embedment depths, in other words, when the pile base is located close to the boundary between a weak upper layer and the founding sand layer. In contrast, the LCPC and adapted filter methods give mean α_p values of around 0.30. Across these two averaging methods, the variation is much smaller and consistent across all embedment depths compared to the 4D/8D and De Beer methods.

The variation suggests that particular care should be taken when using the 4D/8D and De Beer averaging methods for shallow penetration of piles in the founding sand layer. This is in line with reviews (Randolph 2003; White and Bolton 2005) of a driven precast pile database where partial embedment was found to introduce variation and geometrical trends in α_p across the database. The LCPC and adapted filter methods give very similar results for the piles in the database. In general, this similarity can be expected for homogeneous sands, as was the case for the piles in the database. For more variable or interlaminated sand layers, the adapted filter method should be considered (Lehane et al. 2020).

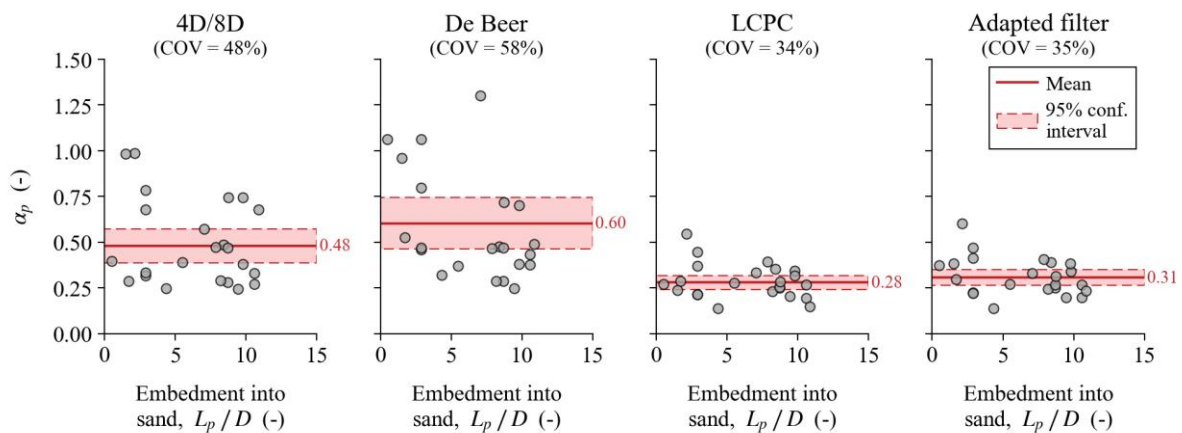


Fig. 12. Variation in α_p using four different methods to determine $q_{c,avg}$.

Influence of pile geometry

When α_p is determined using the LCPC or the adapted filter methods, the database has a coefficient of variation (COV) in α_p of around 35% across all piles. Comparing piles within individual test sites, the within-site variation ranges from 16% (Amaliahaven) to 36% (Zeeland)—for sites where at least three piles were tested. To put these values into context, the COV from other pile databases is 23% for closed-ended driven piles (Xu et al. 2008), 30% for driven cast-in-situ piles (Flynn and McCabe 2021) and 17% for non-displacement piles (Gavin et al. 2013) when using the LCPC averaging method. Patently, the presented screw displacement pile database shows higher variability in α_p when compared to other load test databases.

To investigate the variation further, α_p is compared to the pile length, pile diameter, pile slenderness and $q_{c,LCPC}$ (Fig. 13). Despite the variation in α_p , no clear trend is evident with pile length, pile diameter or pile slenderness. In terms of the design cone resistance $q_{c,LCPC}$, no clear trend is shown between

resistances of 10 to 40 MPa, although more data is needed beyond 40 MPa to confirm the existence or non-existence of any trend.

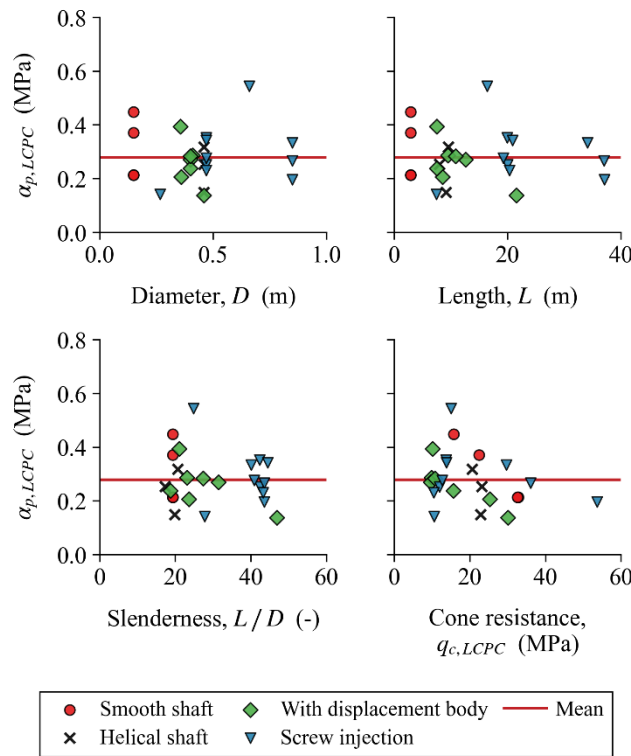


Fig. 13. Variation in α_p with pile geometry and soil conditions.

The database includes a range of pile tip shapes. Not only do these vary across different types of screw displacement piles, but variations also occur within each pile type because of different construction procedures, soil conditions or hydrological conditions. These variations can influence the mobilisation rate and the ultimate value of the pile base resistance (Sharif et al. 2021; Tovar-Valencia et al. 2021). However for almost all test piles in the database, the piles were not extracted after testing and so the true realised shape of each pile is unknown. Consequently, it is likely that some of the variability in the ultimate base resistances can be attributed to differences in realised pile base geometries, incurred by both installation-related effects on the surrounding soil, concrete pouring and casing extraction.

Influence of pile installation

As well as the differences in pile tip geometries, some variation in the base resistances may have been caused by changes in installation procedures. This includes variations not just between different screw displacement pile types, but also within each pile type. Some influencing parameters include the

installation energy, rate of penetration, concreting pressure or the rate of extraction of augers or reusable casings (Bustamente and Gianceselli 1998; Slatter 2000; van Impe 2001). Unfortunately, examining these parameters across the database is not possible because of the lack of installation data reported. Nevertheless, no distinct differences in the mean α_p can be observed across each screw displacement pile category, for instance, between screw displacement piles with grout injection ($\alpha_p = 0.28$) and without grout injection ($\alpha_p = 0.27$) or between those with a helical shaft ($\alpha_p = 0.28$) and those with a smooth shaft ($\alpha_p = 0.24$).

A component also not considered in the database is the influence of residual loads. For cast-in-situ piles, residual loads can develop from volumetric changes in curing concrete and also from the dissipation of excess pore pressures in cohesive soils, inducing a downdrag on the pile (Fellenius 2002; Siegel and McGillivray 2009; Flynn et al. 2012; Krasinski and Wiszniewski 2021). Directly measuring these residual loads is difficult for cast-in-situ piles: firstly, because of the complexity in separating curing-induced strains from mechanically induced strains, and secondly, the constantly changing stiffness of the pile during concrete curing means converting strains to a normal force is not trivial. Nevertheless, no clear trends were observed in α_p when considering the screw injection pile tests at Delft or similar sites (Loenhout, Oostende, Pruszcz and Zulawy) where the pile penetrated through a large amount of soft clay and where downdrag may incur a response at the pile base.

Fig. 14 compares screw displacement piles to a database of bored and CFA piles (Gavin et al. 2013) as well as to a database of driven closed-ended piles with residual loads excluded (Xu et al. 2008; Bittar et al. 2020). The general trend shows that screw displacement piles behave more like a non-displacement pile than a full displacement pile type. Notwithstanding, the high variation in the screw displacement pile database is evident. Part of this variation may be attributed to interpretation uncertainty, for example, when estimating the pile tip geometry and the pile base resistance. However, the variation may also suggest the sensitivity of screw displacement piles to installation, both in terms of the influence of installation on the influence zone around the pile tip as well as the soil-structure interaction mechanisms occurring at the screw tip under loading.

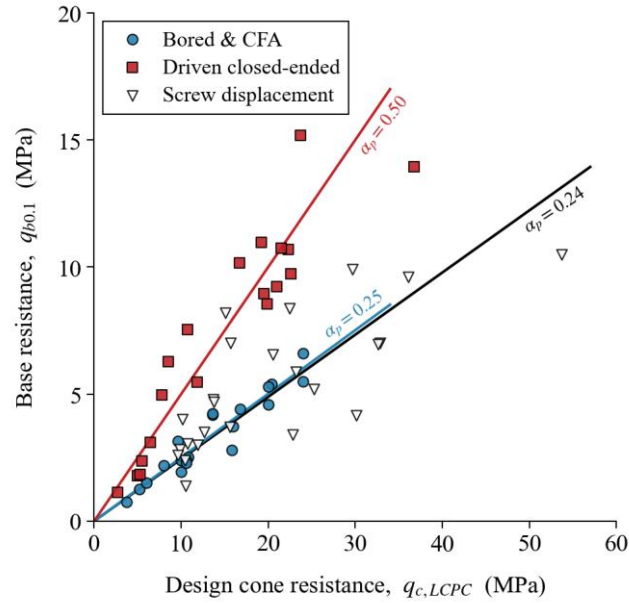


Fig. 14. Screw displacement pile test database compared to non-displacement (Gavin et al. 2013) and full displacement (Xu et al. 2008; Bittar et al. 2020) databases. Residual loads have not been included.

CONCLUSION

Five compression load tests were performed in Delft, the Netherlands, on full-scale screw injection piles (two Fundex and three Tubex piles), installed in soft clay and founded in medium dense to dense sand. Each pile was fully instrumented with distributed fibre optic sensors, showing clearly the base and shaft response of each pile. These measurements showed that the total capacity of two of the three Tubex piles was affected by structural failure of the grout body, resulting in the transfer of load directly to the pile base. All five piles could only mobilise a base capacity roughly 50% of the predicted capacity in different national design standards.

To investigate this further, the study was extended to a database analysis of all types of screw displacement piles. The analysis demonstrated the importance of CPT q_c averaging methods in the derivation of the ultimate base capacity, showing that some averaging methods can be affected by weak soils overlying the pile base. Using the LCPC 1.5D averaging method, the analysis showed that all the screw displacement pile types mobilised base resistances comparable to a soil-replacing pile instead of a fully displacing pile, suggesting that the installation of screw displacement piles leads to little improvement in its base resistance. Nevertheless, large variability in the normalised base resistances

suggests that pile tip shape, concreting procedures and other installation-related effects can have an impact on the pile base response and the interpretation of the test results.

DATA AVAILABILITY STATEMENT

The data presented in this study is available from the corresponding author upon reasonable request.

ACKNOWLEDGMENTS

This research is part of the *InPAD* project, a project funded by *Het Topconsortium voor Kennis en Innovatie (TKI) Deltatechnologie* and seven industry partners: Delft University of Technology, Deltares, Dutch Association of Piling Contractors (NVAF), Dutch Ministry of Infrastructure and Water Management (*Rijkswaterstaat*), Fugro, the Municipality of Rotterdam (*Gemeente Rotterdam*) and the Port of Rotterdam Authority. In addition, the authors are grateful for the financial support of the Dutch Ministry of Infrastructure and Water Management for the Delft pile tests along with the assistance of Fundex Piling Group and APTS during the pile test programme.

NOTATION

The following symbols are used in this paper:

D = pile diameter;

f_s = cone penetration test friction sleeve resistance;

L = pile length;

L_p = pile length embedded in sand;

q_b = pile base resistance;

$q_{b0.1}$ = pile base resistance at a base displacement of 10% of the pile diameter;

q_c = cone penetration test tip resistance;

$q_{c,avg}$ = weighted average of cone tip resistances for determining the pile base resistance;

$q_{c,LCPC} = q_{c,avg}$ determined by the 1.5 LCPC averaging method;

492 q_s = pile shaft resistance;

493 R_f = cone penetration test friction ratio ($= f_s/q_c$);

494 s_b = pile base displacement;

495 u_2 = cone penetration test pore water pressure;

496 α_p = correlation factor for determining the pile base resistance ($= q_{c,avg}/q_b$);

497 REFERENCES

- 498 Admiraal, B. J., S. A. Aguilar, S. Van Dijk, and P. IJnsen. 2022. "Influence of grout injection parameters
499 on shaft bearing capacity of screw displacement piles." *11th Int. Conf. Stress Wave Theory and Design
500 and Testing Methods for Deep Foundations*. Rotterdam, The Netherlands.
501 <https://doi.org/10.5281/zenodo.7139213>
- 502 AFNOR (French Standardisation Association) 2018. *Justification des ouvrages géotechniques - Normes
503 d'application nationale de l'Eurocode 7 - Fondations profondes* [Justification of geotechnical work –
504 National application standards for the implementation of Eurocode 7 – Deep foundations]. [In French.]
505 NF P94-262/A1. Paris, France: AFNOR.
- 506 Ahmadi, M. M., and P. K. Robertson. 2005. "Thin-layer effects on the CPT q_c measurement." *Can.
507 Geotech. J.*, 42 (5), 1302–1317. <https://doi.org/10.1139/t05-036>.
- 508 Basu, P., M. Prezzi, and R. Salgado. 2014. "Modeling of installation and quantification of shaft
509 resistance of drilled-displacement piles in sand." *Int. J. Geomech.*, 14 (2): 214–229.
510 [https://doi.org/10.1061/\(ASCE\)GM.1943-5622.0000303](https://doi.org/10.1061/(ASCE)GM.1943-5622.0000303).
- 511 Basu, P., M. Prezzi, and D. Basu. 2010. "Drilled displacement piles – Current practice and design." *J.
512 Deep Found. Inst.*, 4 (1), 3–20. <https://doi.org/10.1179/dfi.2010.001>.
- 513 de Beer, E. 1971. "Methodes de deduction de la capacite portante d'un pieu a partir des resultats des
514 essais de penetration" [Methods for deducing the bearing capacity of a pile from penetration test
515 results]. [In French] *Annales des Travaux Publics de Belgique*, 1971–2 (4/5 ET 6), 191–268.
- 516 Bittar, E. J., B. M. Lehané, R. W. Boulanger, and J. T. DeJong. 2020. "CPT filter to estimate the end
517 bearing of closed-ended driven piles in layered sands." *Proc. 4th Int. Symp. Front. Offshore Geotech.*,
518 520–528. Austin, Texas, USA: Deep Foundations Institute.
- 519 Bittar, E. J., Y. Tian, and B. M. Lehané. 2022. "Application of a new q_c averaging approach for end
520 bearing of driven piles in sand." *Proc. 5th Int. Symp. Cone Penetration Testing (CPT22)*, 832–837.
521 Bologna, Italy: CRC Press.
- 522 de Boorder, M., D. A. de Lange, and K. G. Gavin. 2022. "An alternative CPT averaging procedure to
523 estimate pile base capacity." *11th Int. Conf. Stress Wave Theory and Design and Testing Methods for
524 Deep Foundations*. Rotterdam, The Netherlands. <https://doi.org/10.5281/zenodo.7142197>.
- 525 Bottiau, M., and N. Huybrechts. 2019. "Recent advances in pile design, construction, monitoring and
526 testing." *Proc. XVII ECSMGE-2019*. Reykjavik, Iceland.
- 527 Boulanger, R. W., and J. T. DeJong. 2018. "Inverse filtering procedure to correct cone penetration data
528 for thin-layer and transition effects." *Proc. 4th Int. Symp. Cone Penetration Testing (CPT18)*. 24–44.
529 Delft, The Netherlands: CRC Press.

530 Bustamente, M., and L. Gianceselli. 1982. "Pile bearing capacity prediction by means of static
531 penetrometer CPT." *Proc. Second Eur. Symp. Penetration Test.*, 493–500. Amsterdam, The
532 Netherlands.

533 Bustamente, M., and L. Gianceselli. 1997. "Portance d'un pieu De Waal, vissé moulé dans un sable sous
534 nappe" [Capacity of a De Waal pile, auger cast in sand under groundwater level]. [In French.] *Bull. des*
535 *Laboratoires des Ponts et Chaussées* 208 (Mar-Apr): 107–115.

536 Bustamente, M., and L. Gianceselli. 1998. "Installation parameters and capacity of screwed piles." *Proc.*
537 *3rd Inter. Geotech. Seminar on Deep Foundations on Bored and Auger Piles (BAP III)*, 95–108. Ghent,
538 Belgium: Balkema.

539 Chin, F. K. 1970. "Estimation of the ultimate load of piles from tests not carried to failure." *Proc 2nd*
540 *Southeast Asian Conf. Soil Eng.*. Singapore.

541 de Cock, F. A. 2008. "Sense and sensitivity of pile load-deformation behaviour." *5th Int. Symp. Deep*
542 *Found. Bored Auger Piles (BAP V)*, 23–44. Ghent, Belgium: CRC Press.

543 Duffy, K. J., K. G. Gavin, M. Korff, D. A. De Lange, and A. A. Roubos. 2024. "Influence of installation
544 method on the axial capacity of piles in very dense sand." *J. Geotech. Geoenvironmental Eng.*
545 <https://doi.org/10.1061/JGGEFK/GTENG-12026>. [Forthcoming].

546 Fellenius, B. H. 2002. "Determining the resistance distribution in piles. Part 2: Method for determining
547 the residual load." *Geotech. News Mag.*, 20 (3), 25–29.

548 Figueroa, G., A. Marinucci, and A. Lemnitzer. 2022. "Axial load capacity predictions of drilled
549 displacement piles with SPT- and CPT-based direct methods." *J. Deep Foundations Inst.*, 16 (2).
550 <https://doi.org/10.37308/DFIJnl.20220512.262>.

551 Flynn, K. N., and B. A. McCabe. 2021. "Applicability of CPT Capacity Prediction Methods to Driven
552 Cast-In-Situ Piles in Granular Soil." *J. Geotech. Geoenvironmental Eng.*, 147 (2): 04020170.
553 [https://doi.org/10.1061/\(ASCE\)GT.1943-5606.0002445](https://doi.org/10.1061/(ASCE)GT.1943-5606.0002445).

554 Flynn, K. N., B. A. McCabe, and D. Egan. 2012. "Residual load development in cast-in-situ piles – a
555 review and new case history." *Proc. 9th Int. Conf. Testing and Design Methods for Deep Foundations*,
556 765–773. Kanazawa, Japan.

557 Gavin, K., D. Cadogan, A. Tolooiyan, and P. Casey. 2013. "The base resistance of non-displacement
558 piles in sand. Part I: field tests." *Proc. Inst. Civ. Eng. - Geotech. Eng.*, 166 (6), 540–548.
559 <https://doi.org/10.1680/geng.11.00100>.

560 Gavin, K., M. S. Kovacevic, and D. Igoe. 2021. "A review of CPT based axial pile design in the
561 Netherlands." *Undergr. Space*, 6 (1), 85–99. <https://doi.org/10.1016/j.undsp.2019.09.004>.

562 Geerling, J., and E. Janse. 1992. "Proefbelastingen op schroefinjectiepalen te Rosmalen" [Pile tests on
563 screw injection piles in Rosmalen]. [In Dutch.]. Grondmechanica Delft.

564 van der Geest, A. J., B. J. Admiraal, and P. IJnsen. 2020. "Schaalproeven op draagvermogen
565 grondverdringende (schroef)palen" [Scaled tests on the bearing capacity of ground displacing (screw)
566 piles]. [In Dutch.]. *Geotechniek*, (June 2020), 7–16.

567 Hijma, M. P., K. M. Cohen, W. Roebroeks, W. E. Westerhoff, and F. S. Busschers. 2012. "Pleistocene
568 Rhine–Thames landscapes: geological background for hominin occupation of the southern North Sea
569 region." *J. Quaternary Sciencs*, 27 (1), 17–39. <https://doi.org/10.1002/jqs.1549>.

570 Huybrechts, N. 2001. "Test campaign at Sint-Katelijne-Waver and installation techniques of screw
571 piles." *Proc. Symp. Screw Piles*. 151–204. Brussels, Belgium: AA Balkema.

572 Huybrechts, N., V. Whenham. 2003. "Pile testing campaign on the Limelette test site and installation
573 techniques of screw piles." *Proc. 2nd Symp. on Screw Piles*. 71–130. Brussels, Belgium: CRC Press.

574 Huybrechts, N., M. De Vos, M. Bottiau, and L. Maertens. 2016. "Design of piles—Belgian practice."
575 *Proc. ISSMGE–ETC3 Int. Symp. on Design of Piles in Europe*, 7–44. Leuven, Belgium.

576 van Impe, W. F. 2001. "Considerations on the influence of screw pile installation parameters on the
577 overall pile behaviour." *Proc. Symp. Screw Piles*. 127–150. Brussels, Belgium: AA Balkema.

578 van Impe, P. O., W. F. Van Impe, and L. Seminck. 2013. "Discussion of an instrumented screw pile
579 load test and connected pile group load settlement behavior." *J. Geo-Eng. Sci.*, 1 (1), 13–36.
580 <https://doi.org/10.3233/JGS-130011>.

581 Jeffrey, J. 2012. *Investigating the performance of continuous helical displacement piles*. PhD Thesis.
582 Dundee, United Kingdom: University of Dundee.

583 Kempfert, H.-G., and P. Becker. 2010. "Axial pile resistance of different pile types based on empirical
584 values." *GeoShanghai 2010 - Deep Found. Geotech. Situ Test.*, 149–154. Shanghai: ASCE.

585 Knappett, J. A., K. Caucis, M. J. Brown, J. R. Jeffrey, and J. D. Ball. 2016. "CHD pile performance:
586 part II – numerical modelling." *Proc. Inst. Civ. Eng. - Geotech. Eng.*, 169 (5), 436–454.
587 <https://doi.org/10.1680/jgeen.15.00132>.

588 Krasiński, A. 2011. "Badania terenowe przemieszczeniowych pali i kolumn wkręcanych typu SDP i
589 SDC" [Field tests of displacement piles and screwed SDP and SDC columns]. [In Polish.] *Drogi I*
590 *Mosty*, (1–2): 21–58.

591 Krasiński, A. 2023. "Estimation of screw displacement pile-bearing capacity based on drilling
592 resistances." *Studia Geotechnica et Mechanica*, 45 (S1), 1–11. <https://doi.org/10.2478/sgem-2023-0014>.
593 [0014](https://doi.org/10.2478/sgem-2023-0014).

594 Krasiński, A., and M. Wiszniewski. 2021. "Estimation of screw displacement pile-bearing capacity
595 based on drilling resistances." *Studia Geotechnica et Mechanica*, 45 (S1), 1–11.
596 <https://doi.org/10.2478/sgem-2023-0014>.

597 de Lange, D. A., 2018. "CPT in thinly layered soils: validation tests and analysis for multi thin layer
598 correction." *Rep. No. 1209862-006-GEO-0007*, Deltares, the Netherlands.

599 Larisch, M. 2014. *Behaviour of stiff, fine-grained soil during the installation of screw auger*
600 *displacement piles*. PhD Thesis. Brisbane, Australia: The University of Queensland.

601 Lehane, B.M. 2019. "CPT-based design of foundations. E.H. Davis Memorial Lecture." *Australian*
602 *Geomechanics Journal*, 54 (4), 23–48.

603 Lehane, B. M., Z. Liu, E. Bittar, F. Nadim, S. Lacasse, R. J. Jardine, P. Carotenuto, M. Rattley, P.
604 Jeanjean, K. G. Gavin, R. Gilbert, J. Bergan-Haavik, and N. Morgan. 2020. "A new 'unified' CPT-
605 based axial pile capacity design method for driven piles in sand." *Proc. 4th Int. Symp. Front. Offshore*
606 *Geotech.*, 462–477. Austin, Texas, USA: Deep Foundations Institute.

607 van der Linden, T. I., D. A. de Lange, and M. Korff. 2018. "Cone penetration testing in thinly inter-
608 layered soils." *Proc. Inst. Civ. Eng. - Geotech. Eng.*, 171 (3), 215–231.
609 <https://doi.org/10.1680/jgeen.17.00061>.

610 Meyerhof, G. G. 1959. "Compaction of sands and bearing capacity of piles." *J. Soil Mech. Found.*
611 *Division*, 85(6), 1–29. <https://doi.org/10.1061/JSFEAQ.0000231>.

612 van Mierlo, W., and A. Koppejan. 1952. "Lengte en draagvermogen van heipalen" [Length and bearing
613 capacity of driven piles]. [In Dutch.] *Bouw*, 3.

614 Moshfeghi, S., and A. Eslami. 2019. "Reliability-based assessment of drilled displacement piles bearing
615 capacity using CPT records." *Marine Georesources Geotechnol.*, 37 (1), 67–80.
616 <https://doi.org/10.1080/1064119X.2018.1448493>.

617 NBN (Belgian Bureau of Normalisation). 2022. Eurocode 7 : Geotechnisch ontwerp - Deel 1 :
618 Algemene regels [Eurocode 7: Geotechnical design – Part 1: General rules]. [In Dutch.] NBN EN 1997-
619 1 ANB:2022. Brussels, Belgium: NBN

620 NEN (Dutch Standardisation Institute). 2017. *Geotechnisch ontwerp van constructies - Deel 1:*
621 *Algemene regels* [Geotechnical design of structures – Part 1: General rules]. [In Dutch.] NEN 9997-
622 1+C2. Delft, The Netherlands: NEN.

623 NeSmith, W. M. 2002. “Design and installation of pressure-grouted, drilled displacement piles.” *Proc.*
624 *9th Int. Conf. Piling Deep Foundations*. Nice, France: Deep Foundations Institute.

625 Park, S., L. A. Roberts, and A. Misra. 2012. “Design methodology for axially loaded auger cast-in-
626 place and drilled displacement piles.” *J. Geotech. Geoenvironmental Eng.*, 138 (12), 1431–1441.
627 [https://doi.org/10.1061/\(ASCE\)GT.1943-5606.0000727](https://doi.org/10.1061/(ASCE)GT.1943-5606.0000727).

628 Pucker, T., and J. Grabe. 2012. “Numerical simulation of the installation process of full displacement
629 piles.” *Comput. Geotech.*, 45, 93–106. <https://doi.org/10.1016/j.compgeo.2012.05.006>.

630 Randolph, M. F. 2003. “Science and empiricism in pile foundation design.” *Géotechnique*, 53 (10),
631 847–875. <https://doi.org/10.1680/geot.2003.53.10.847>.

632 Reinders, K., A. van Seters, and M. Korff. 2016. “Design of piles according to Eurocode 7 – Dutch
633 practice.” *Proc. ISSMGE - ETC 3 Int. Symp. Des. Piles Eur.*. Leuven, Belgium.

634 Rijdsdijk, K. F., S. Passchier, H. J. T. Weerts, C. Laban, R. J. W. van Leeuwen, and J. H. J. Ebbing.
635 2005. “Revised Upper Cenozoic stratigraphy of the Dutch sector of the North Sea Basin: towards an
636 integrated lithostratigraphic, seismostratigraphic and allostratigraphic approach.” *Neth. J. Geosci.*, 84
637 (2): 129–146. <https://doi.org/10.1017/S0016774600023015>.

638 van Seters, A. 2016. “General Report – Calculation methods based on direct derivation from in situ
639 tests.” 31–45. *Proc. ISSMGE - ETC 3 Int. Symp. Des. Piles Eur.*. Leuven, Belgium.

640 Sharif, Y. U., M. J. Brown, B. Cerfontaine, C. Davidson, M. O. Ciantia, J. A. Knappett, J. D. Ball, A.
641 Brennan, C. Augarde, W. Coombs, A. Blake, D. Richards, D. White, M. Huisman, and M. Ottolini.
642 2021. “Effects of screw pile installation on installation requirements and in-service performance using
643 the discrete element method.” *Can. Geotech. J.*, 58 (9): 1334–1350. <https://doi.org/10.1139/cgj-2020-0241>.

645 Siegel, T. C., T. J. Day, B. Turner, and P. Faust. 2019. “Measured end resistance of CFA and drilled
646 displacement piles in San Francisco Area alluvial clay.” *J. Deep Foundations Inst.*, 12 (3), 186–189.

647 Siegel, T. C., and A. McGillivray. 2009. “Interpreted residual load in an augered cast-in-place pile.”
648 *Proc. 34th Annu. Conf. Deep Foundations*, 173–182. Deep Foundations Institute.

649 Slatter, J. W. 2000. *The fundamental behaviour of displacement screw piling augers*. PhD Thesis.
650 Melbourne, Australia: Monash University.

651 Tehrani, F. S., M. I. Arshad, M. Prezzi, and R. Salgado. 2018. “Physical modeling of cone penetration
652 in layered sand.” *J. Geotech. Geoenvironmental Eng.*, 144 (1), 04017101.
653 [https://doi.org/10.1061/\(ASCE\)GT.1943-5606.0001809](https://doi.org/10.1061/(ASCE)GT.1943-5606.0001809).

654 Theys, F., J. Maertens, and W. Maekelberg. 2003. “Practical experience with screw piles used for the
655 high-speed railway in Belgium.” *Proc. Second Symp. Screw Piles*, 235–271. Brussels, Belgium: CRC
656 Press.

657 Tovar-Valencia, R. D., A. Galvis-Castro, R. Salgado, and M. Prezzi. 2021. “Effect of base geometry on
658 the resistance of model piles in sand.” *J. Geotech. Geoenvironmental Eng.*, 147 (3): 04020180.
659 [https://doi.org/10.1061/\(ASCE\)GT.1943-5606.0002472](https://doi.org/10.1061/(ASCE)GT.1943-5606.0002472).

- 660 Verheyde, F.A. and F. Baguelin. 2019. "Pile design using CPT results: the "LPC method"." *Proc. 13th*
661 *Australia New Zealand Conf. Geomech.*, 421–426. Sydney, Australia: Australian Geomechanics
662 Society.
- 663 White, D. J., and M. D. Bolton. 2005. "Comparing CPT and pile base resistance in sand." *Proc. Inst.*
664 *Civ. Eng. - Geotech. Eng.*, 158 (1): 3–14. <https://doi.org/10.1680/geng.2005.158.1.3>.
- 665 Xu, X., and B. M. Lehane. 2008. "Pile and penetrometer end bearing resistance in two-layered soil
666 profiles." *Géotechnique*, 58 (3), 187–197. <https://doi.org/10.1680/geot.2008.58.3.187>.
- 667 Xu, X., J. A. Schneider, and B. M. Lehane. 2008. "Cone penetration test (CPT) methods for end-bearing
668 assessment of open- and closed-ended driven piles in siliceous sand." *Can. Geotech. J.*, 45 (8), 1130–
669 1141. <https://doi.org/10.1139/T08-035>.